Localization of Electromagnetic Interference Sources Using a Time Reversal Cavity

Hamidreza Karami, Mohammad Azadifar, *Member, IEEE,* Amirhossein Mostajabi, *Student Member, IEEE,* Pierre Favrat, Marcos Rubinstein, *Fellow IEEE*, Farhad Rachidi, *Fellow, IEEE*

Abstract— In this paper, we propose and implement a novel technique to locate Electromagnetic Interference (EMI) sources using the concept of time reversal cavity. We show in an intuitive manner that reflections from the surfaces of a cavity can emulate an infinite number of sensors in the Time Reversal (TR) method. In order to locate EMI sources, the equipment under test (EUT) is placed in a rectangular metallic cavity, of suitable dimensions according to the considered frequency band and the EUT size, equipped with a simple monopole or dipole antenna. We demonstrate that, by using only one sensor, we are able to locate EMI sources by taking advantage of the focusing properties of a time reversal cavity. The entropy criterion is applied to obtain the focusing time slice in which the maximum electric field determines the location of the EMI source. Both two- and three-dimensional numerical simulation schemes are deployed to demonstrate the ability of the proposed technique. The validity of numerical simulations is tested against frequency domain measurements. Compared to conventional EMI tests in anechoic chambers and scanning methods, the proposed technique represents a simpler and cost-effective test method requiring only one sensor (a monopole or dipole antenna).

***Index Terms*— Cavity, Electromagnetic Interference, Entropy Source Localization, Time Reversal.**

I. Introduction

The dimensions of electronic circuit boards are becoming smaller and smaller to achieve larger bandwidths and higher data transfer speeds. This, in turn, is leading to an increase in the level of Electromagnetic Interference (EMI) from electronic circuit boards [1]. Anechoic, semi-anechoic (based on CISPR 22 and IEC 61000-6 standards) and reverberation chambers are used to measure the level of EMI radiation of EUTs. These tests are expensive, and they are associated with difficulties in terms of installation, operation, and maintenance. In addition, the localization of EMI sources cannot be performed via these test procedures.

Source localization techniques are used in many applications, such as, wireless communications [2], wireless sensor networks [3], radar [4], sonar [5], seismology [6], acoustics [7], industrial electronics [8]–[10], electromagnetic compatibility [11], and lightning [12]. Near-field electromagnetic scanning methods are the main tools to locate EMI sources (e.g. [13], [14]). However, the presence of evanescent waves at close distances may cause faulty reconstruction of the source. Moreover, the need for accessibility of all onboard locations and the positioning of the probe are also fundamental limitations of these methods. The Emission Source Microscopy (ESM) technique was proposed by Maheshwari et al. as a far-field scanning method to overcome the limitations of near-field scanning methods [15]. However, the ESM technique can only be applied to planar source structures and a scan must be performed over the plane of observation.

The time reversal method is a source localization algorithm with demonstrated ability to provide wave focusing in complex and heterogeneous media both in time and space [16], [17]. In the time reversal method, the radiation from the disturbance source is measured by one or several sensors which back-inject a time-reversed version of the measured waveform by flipping the signal in time. The back-injected signal focuses at the original disturbance source's location by virtue of the time reversal symmetry of the wave equation [11]. The accuracy of the time reversal method is improved by multiple scattering in the location domain [18]. As a result, a great deal of attention has been given to the application of the TR method in reverberation chambers. In this respect, a theoretical model for Time Reversal Cavities (TRCs) was established for ultrasound by Cassereau and Fink [19], who found that TRCs can create focal spots with a limited number of sensors. Source reconstruction can be achieved in an acoustic cavity using only one transceiver [20]. In the following works by Fink and co-workers ([21], [22]), the focusing property of TRCs for electromagnetic waves was proven both experimentally and theoretically. TRCs have also been utilized to perform electromagnetic susceptibility (EMS) tests [23], [24].

In this paper, we propose a novel approach to localize EMI sources based on the time reversal process. The device under test (DUT) is placed inside a metallic cavity and a single dipole antenna is used to record the EMI, which is then used to localize the EMI source.

We investigate the application of the time reversal technique by going from the simple case of a 2D model to the more practical case of a 3D cavity, pointing out insights for each one of the studied cases. The organization of the paper is as follows.

H. Karami, A. Mostajabi, and F. Rachidi are with the École polytechnique fédérale de Lausanne, Lausanne 1015, Switzerland (e-mail: hamidreza.karami@epfl.ch; amirhossein.mostajabi@epfl.ch; farhad.rachidi@epfl.ch).

M. Azadifar, P. Favrat and M. Rubinstein are with the Institute for Information and Communication Technologies, Haute Ecole d'ingénierie et de Gestion du Canton de Vaud, Yverdon-les-bains 1401, Vaud, Switzerland. (e-mail: mohammad.azadifar@heig-vd.ch; rubinstein.m@gmail.com).

This article has been accepted for publication in a future issue of this journal, but has not been fully edited. Content may change prior to final publication. Citation information: DOI 10.1109/TIE.2019.2962460, IEEE Transactions on Industrial Electronics

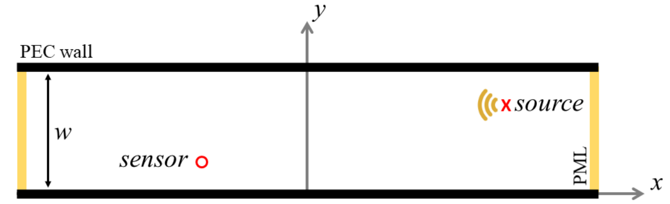

Fig. 1. Parallel plate waveguide (PPW). Direct Time solution including a sensor and a source. In 2D-FDTD simulations, two PMLs are used to model the infinite length PEC walls along the *x*-axis.

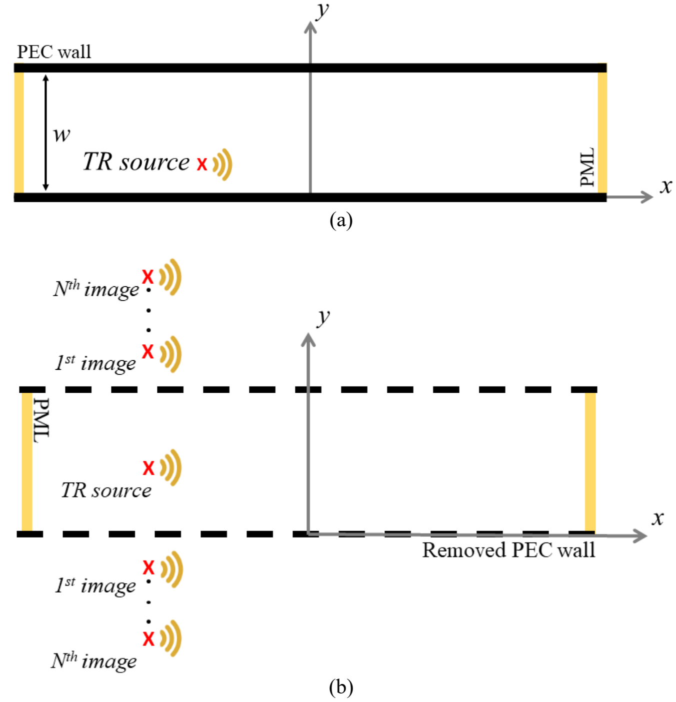

Fig. 2. Parallel plate waveguide (PPW). Reverse Time solution. a) Original problem, b) equivalent problem. Note that the sensor in Fig. 1 has turned into the source for the back propagation represented in this figure.

In Section II, we propose a new perspective on the TRC concept based on the use of image theory. We illustrate in that section that the ability of TR to locate sources using a single sensor emerges from the fact that the single sensor gives rise to multiple images that act as additional sensors. In Section III, we test the ability of the proposed method to locate EMI sources in 2D problems. In Section IV, we validate our simulation scheme and we tackle the practical problem of an EMI source in a PCB in a rectangular cavity. Finally, Section V is devoted to general conclusions.

II. Time Reversal Cavity: A New Perspective Using Image Theory

In this section, we present an intuitive explanation, using image theory, to show that the problem of source localization in a parallel plate structure with a single sensor is electromagnetically equivalent to the problem of source localization with an infinite number of sensors in free space. The infinite number of sensors can provide the exact EMI source location. This concept can be easily extended to full cavities. We first provide the theoretical basis of the problem and we then validate the procedure via numerical simulations.

A. Theoretical Explanation

The general process of determining the source location using the time reversal method includes the following steps: first, capturing the emitted wave from one or several sources with one or several sensors (in this paper, we use a single sensor). This will be referred to as the forward time step. Second, processing the captured signal to time-reverse it. Third, back-injecting the time-reversed signal into the medium. This third step is referred to as the back-propagation step. In the fourth and last step, to locate the source position, a criterion is applied to obtain the proper source location based on the fact that the waves will refocus both in time and space at the primary source location. The time reversal invariance of the governing wave equation in lossless media guarantees that, for every outgoing wave from a source, the set of back-injected waves converges back to the source [27].

An ideal electromagnetic time reversal process needs an infinite number of sensors to record the signal from the source in the forward time. All of the recorded signals must then be time reversed and back injected into the reciprocal medium.

Without loss of generality, let us consider a parallel plate waveguide (PPW) as shown in Fig. 1, including one source and one sensor. The length of the PPW along the *x* and *z* axes is infinite and its plate separation along the *y* axis is *w*. Both surfaces are considered as perfect electric conductors (PEC) and the dielectric between them is air. To use the TR focusing property in the waveguide, we confine ourselves to the range of frequencies at which the cavity can be considered as electrically large, in other words when *w* is much greater than lambda [26]. The location of the source and sensor are assumed arbitrary.

In the back-propagation step, one can solve two equivalent problems to find the focusing point, depicted, respectively, in Figs. 2a and 2b. In Fig. 2b, the dashed lines show the former locations of the PEC plates in the PPW, which are replaced based on image theory by equivalent sources placed at appropriate locations to account for the PEC. Note that the sensor in the forward time step in Fig. 1 has turned into a source for the back propagation in Fig. 2 and it is marked with a cross (X) in Fig. 2a. As shown in Fig. 2b, by applying image theory, the single-sensor cavity configuration is equivalent to an infinite number of sensors in free space. The image sources produce EM waves that can be considered as the reflections of the original signal from the surfaces of the PPW. All wave fronts will focus at the primary source location at a focusing time based on the TR concept. The time focusing slice is determined using the entropy criterion [25] that will be explained later. Equation (1) can be used to calculate the location of the image sources:

$$Y_i = |y_0| + 2wi \tag{1}$$

where Y_i is the location of the image sources along the *y*-axis, y_0 is the location of the source inside the PPW, *w* is the length of the PPW, and *i* is an integer in the range of $(-\infty, \infty)$.

B. Numerical Validation

In this section, numerical simulations are performed to

This article has been accepted for publication in a future issue of this journal, but has not been fully edited. Content may change prior to final publication. Citation information: DOI 10.1109/TIE.2019.2962460, IEEE Transactions on Industrial Electronics

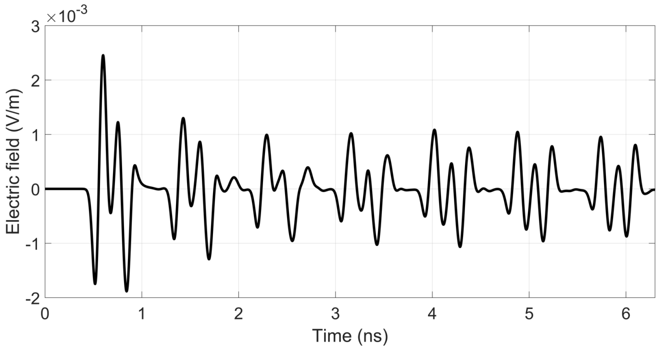

Fig. 3. The signal recorded by the sensor in the forward time.

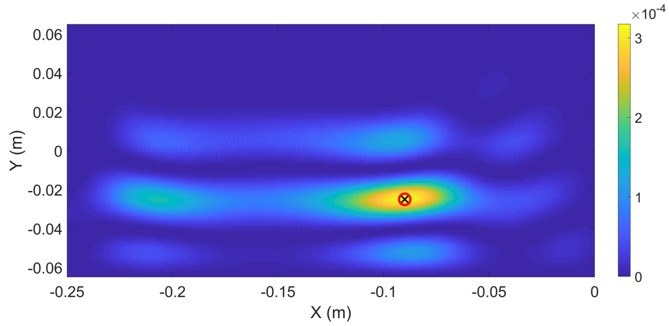

Fig. 4. Distribution of the electric field power over the PPW structure at the optimal time obtained using the minimum entropy criterion.

demonstrate the concept of an infinite number of sensors in a PPW. Fig. 1 shows the geometry of the problem.

We assume a PPW structure with distance of w = 13 cm between the two plates. In our 2D-FDTD model, two Perfectly Matched Layers (PML) are used as boundary conditions to take into account the infinite length of the PPW along the x axis as shown in Fig. 1. Equally spaced cells are used to mesh the solution space. The dimension of each cell is 1×1 mm^2. The time step in this simulation is approximately 2.12 ps.

In the first step (forward time), a Gaussian pulse with a bandwidth of 15 GHz is used as the EMI source. The emitted field is recorded at the location of the sensor (see Fig. 1). The signal recorded by the sensor in the forward time is shown in Fig. 3. In the second step, the signal recorded by the sensor is time-reversed and back-injected into the PPW structure. At this point, we solve the back-propagation problem in two ways: 1) in the presence of the PPW structure and, 2) using image sources (as illustrated in Fig. 2b). In this second way, the PEC walls shown in Fig. 1 are removed and a number of image sources are placed according to Fig. 2b. The location of each image source is determined by (1). One can also see in a more intuitive way where the image sources need to be placed by noting that, while each one of the images helps satisfy the boundary conditions at one of the walls, it requires itself a new image with respect to the other wall. This process repeats indefinitely, with each successive image requiring a new image. Since each new image is farther from the walls than the previous one, and since the fields from the new image decrease very rapidly, the process of adding new images can be truncated with a bound error.

The signal obtained in the forward time is time reversed and back injected from each individual image source. The onset times for all the image sources are the same. The constructive interference of the waves from the image sources will lead to the focusing of the wave at the primary source location. Increasing the number of image sources leads to a better estimation of the source location. Both approaches are implemented using 2D-FDTD simulations.

The entropy values over time can be calculated by (2).

$$R(E_z^n) = \frac{\left[\sum\sum_{j,k}(E_z^n(j,k))^2\right]^2}{\sum\sum_{j,k}(E_z^n(j,k))^4} \tag{2}$$

Fig. 4 and Fig. 5 show the simulation results using the two equivalent problems described in Section II-A, respectively. As shown in Fig. 4, the electric field focuses at the primary source location with an accuracy better than the mesh cell length (1 mm) in the optimal time slice obtained using the entropy criterion. The reason for this focusing is the many reflections from the PPW surfaces.

To show that the multiple reflections from the PPW surfaces are equivalent to an infinite number of sensors, the electric field distribution corresponding to the second problem (described in Fig. 2b) is depicted in Fig. 5. The two closely spaced red dashed lines in Figs. 5a and 5b show the position of the parallel plates in the PPW. In the figure, the black cross (×) between the plates as well as the black crosses above and below the waveguide represent the estimated source locations. The red circles (O) inside the waveguide mark the position of the actual source.

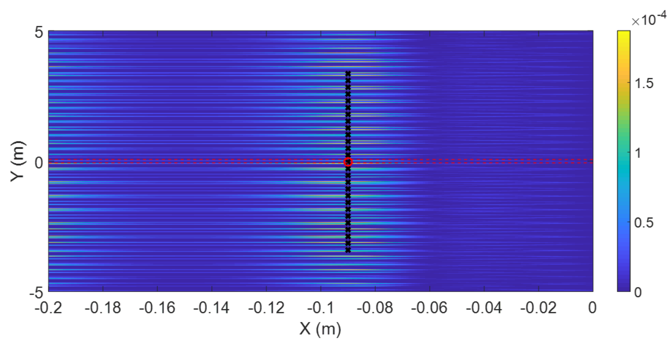

(a)

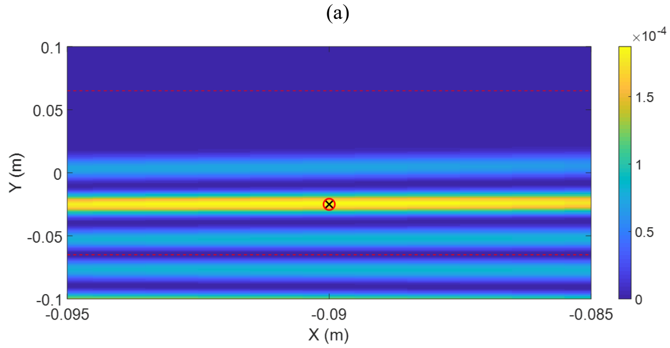

(b)

Fig. 5. Distribution of the electric field power over the equivalent structure based on image theory at the optimal time obtained using the minimum entropy criterion. (a) The whole structure, (b) expanded view. The two closely spaced red dashed lines in Figs. 6a and 6b show the position of the parallel plates in the PPW. In the figure, the black cross between the plates as well as the black crosses above and below the waveguide represent the estimated source locations. The red circles inside the waveguide mark the position of the actual source.

This article has been accepted for publication in a future issue of this journal, but has not been fully edited. Content may change prior to final publication. Citation information: DOI 10.1109/TIE.2019.2962460, IEEE Transactions on Industrial Electronics

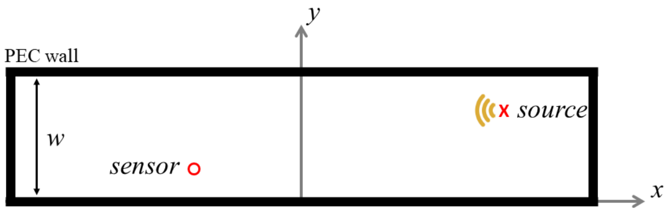

Fig. 6. Full Cavity: Geometry of the 2D problem, including a metallic cavity (thick black PEC frame), one source and one sensor.

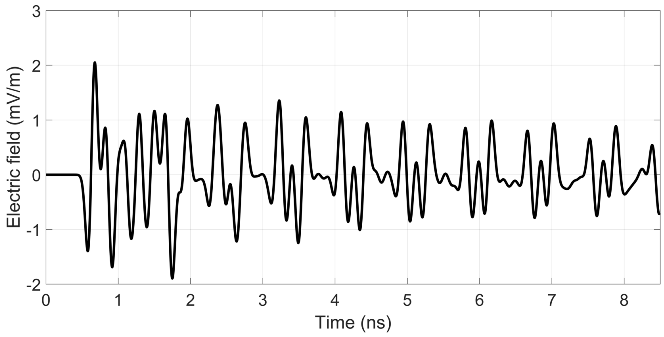

Fig. 7. Recorded electric field by the sensor in the cavity shown in Fig. 6 in the forward time phase.

This shows that the concept of infinite number of images is equivalent to many reflections from the surfaces of the PPW structures. As it can be seen, both methods can detect the exact location of the source. It should be noted that, in the second problem, the first 80 image sources were considered. Crosses (×) show the maximum value of the electric field power at the optimum time slice. As expected, the number of candidate points for the source location is more than one. However, only one of the points is between the PPW plates and it is thus recognized as the correct source location. Other fictitious source locations are repeated periodically above and below the PPW. These locations are only mathematical solutions resulting from the use of images and they are disregarded.

The above-mentioned idea can be easily extended from an ideal infinite PPW structure to a real 3-dimensional cavity. In this case, the sensors are periodically repeated in the three-dimensional space. As we will see, as in the PPW simulation, multiple candidate source locations are found in the 3D cavity problem and only the actual location is confined between the cavity walls.

III. Ability of TRCs to Locate EMI Sources in 2D Problems

In this section, we apply the time reversal method to a one-sensor cavity configuration in a 2D problem using the entropy criterion [12], [25]. Using a 2D-FDTD simulation, we evaluate the ability of the proposed method to locate EMI sources using a single sensor in 2D problems. We consider two cases: a full cavity and a partially open cavity and we apply in each one the TRC concept to locate EMI sources in them.

1) Full Cavity

The geometry of the problem, including a 2D rectangular cavity (25×13 cm^2), one source, and one sensor is shown in Fig. 6. In the forward time step, a Gaussian pulse with a bandwidth

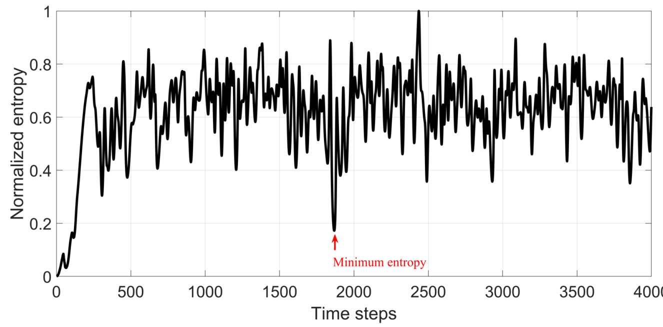

Fig. 8. Entropy of the electric field as a function of time steps for the full cavity structure shown in Fig. 6.

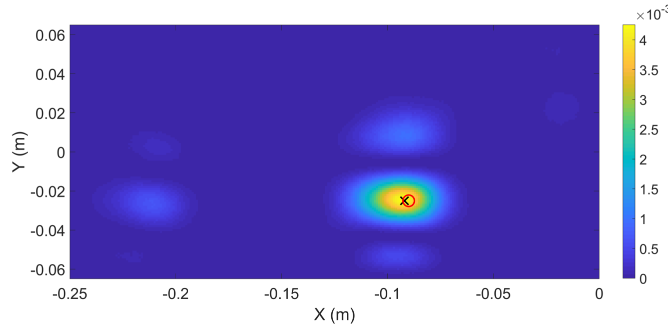

Fig. 9. Distribution of the electric field power at the focusing time slice. The red circle and the black cross represent the actual and the estimated locations of the source, respectively.

of 15 GHz is used as the source and the field at the location of the sensor is recorded. The sensor and source positions are, respectively, (0.035 m, +0.04 m) and (-0.025 m, 0.115 m). The origin and the axes of the selected coordinate system can be seen in Fig. 6. The signal recorded by the sensor in the forward time is shown in Fig. 7. In the second step, the signal recorded at the sensor location is time-reversed and back-injected into the medium. In order to obtain the proper focusing in time and space, we utilize the local minimum entropy criterion as suggested by [12] and [28] and we apply it to our 2D simulations. The formula to obtain the entropy is given in Equation (2). The plot of the entropy over time is depicted in Fig 8.

A discussion on the selection of the proper time slice from the entropy criterion is in order. The minimum entropy criterion was originally applied in image processing to determine spots in an image [25]. In our case, this criterion is used to locate focal spots. With reference to the entropy curve in Fig. 8, the first minimum at t=0 corresponds to the launch of the back propagation at the sensor. Since we have direct knowledge of the sensor location, we can neglect that particular focal spot. The following minima correspond to focal spots resulting from multiple reflections, and the global minimum (apart from the first one, which we have already disregarded) corresponds to the instant at which the back-propagated waves focus back to the source. To the best of our knowledge, this is the first time that the entropy criterion is used for a cavity structure and that it is shown that the global minimum, excluding the beginning of the signal, represents the location of the true source. Once the proper time slice has been found using (2), we search the location domain for the maximum electric field at that time slice

This article has been accepted for publication in a future issue of this journal, but has not been fully edited. Content may change prior to final publication. Citation information: DOI 10.1109/TIE.2019.2962460, IEEE Transactions on Industrial Electronics

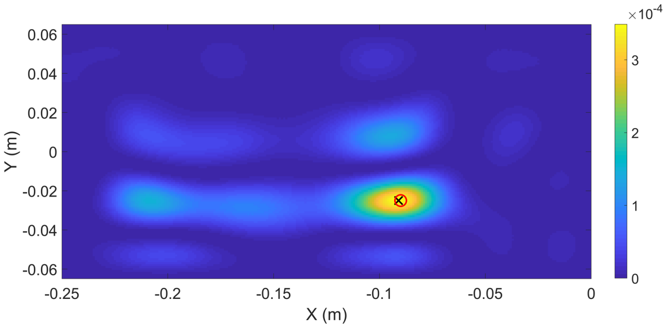

Fig. 10. Distribution of electric field power at the focusing time slice in the partially open cavity. The red circle and the black cross represent the actual and the estimated locations of the source, respectively.

to locate the source. Fig. 9 shows the distribution of the electric field peak power inside the cavity at the focusing time slice. As it can be seen, the location of the source is obtained with an excellent accuracy (less than 2 mm).

2) *Partially Open Cavity*

To further investigate the focusing property of TRCs, we now open the left side of the cavity presented in Fig. 6 and we perform the time reversal process as done for the full cavity. If the image theory method is employed, the multiple images of the sensor repeat only in the y-direction. Therefore, we would expect the quality of the TRC decrease. By applying the time reversal process and using the entropy criterion, the source location can be estimated as shown in Fig. 10. It can be seen that the partially open cavity can still provide accurate results. However, comparing Fig. 9 and Fig. 10, it can be seen that the partially open cavity results in a more diffused focal spot along the *x*-axis. This is essentially because, in this case, the multiple images of the sensor repeat only in the y-direction. However, the accuracy is less than 2 mm, not different from the one obtained in the previous case.

Summarizing the results obtained with the simulations presented in the previous sections, an EMI source can be readily and accurately localized using the concept of TRCs in the presented 2D-problems.

IV. Application of TRCs to Locate EMI Sources in 3D Problems

In the next sections, we investigate the application of the technique to a realistic 3D problem. We utilize the CST-MWS commercial software, which is based on the finite integration technique in the time domain, to simulate the 3D EMI source localization scenarios.

A rectangular cavity with copper walls was considered with dimensions of 25×13×17.4 cm^3. Note that the cross-section of the real cavity is exactly equal to that of the 2D cases studied before. In order to validate our simulation procedure in CST-MWS, we compare in Section IV-1 the transfer function (scattering parameter) of our problem obtained by simulation with CST with the same transfer function obtained via measurement. The verification of the transfer function validates the simulation procedure for both, the forward and backward time phases by virtue of the reciprocity theorem.

In sections IV-2 and IV-3, respectively, the EMI source

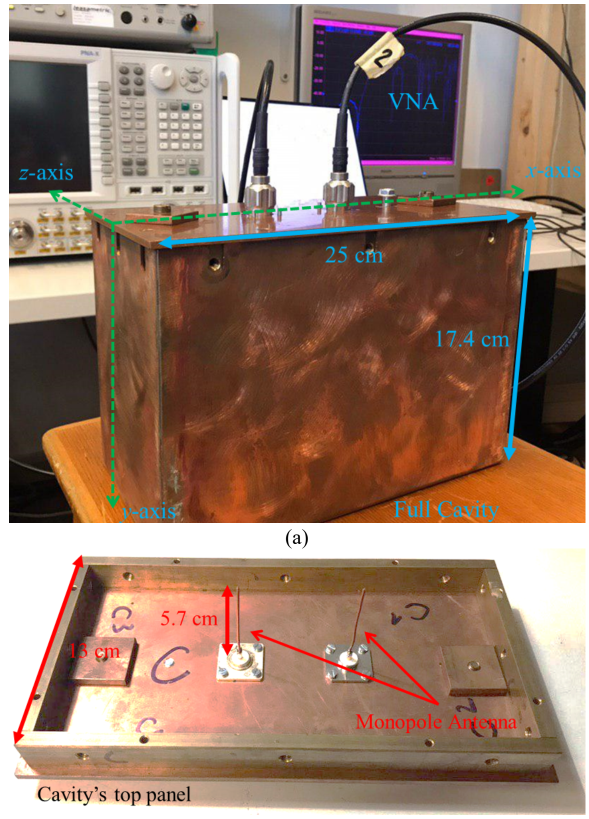

Fig. 11. Experimental Setup. a) A picture of the considered cavity. b) Picture of the interior part of the cavity's top panel including the monopole antennas.

localization problem is solved for a simple monopole EMI source and a large microstrip printed circuit board (PCB) with a total of 24 elements.

1) *Verification of the Simulation Scheme*

In this subsection, we present experimental and simulation results obtained with the real cavity that will be used in the rest of the cases to be presented. The frequency response of the cavity is measured using a Vector Network Analyzer (VNA) and also calculated by simulation using a simple model in CST-MWS. We verify our simulation scheme by comparing these two results. Our test setup includes a rectangular cavity, two monopole antennas with a length of 5.7 cm mounted on a wall of the cavity, and a 9 kHz to 3 GHz VNA.

A picture of the experimental setup is depicted in Fig. 11.

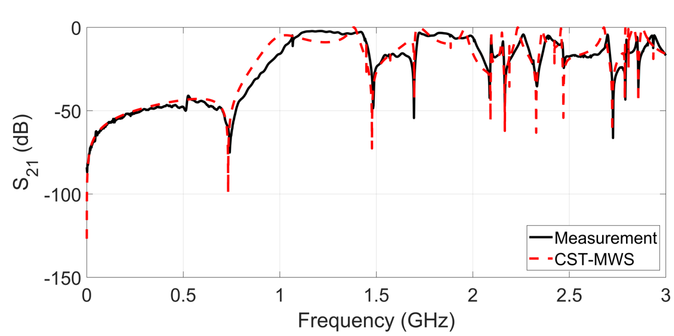

Fig. 12. Comparison between experimental data and simulation results for S_{21}.

This article has been accepted for publication in a future issue of this journal, but has not been fully edited. Content may change prior to final publication. Citation information: DOI 10.1109/TIE.2019.2962460, IEEE Transactions on Industrial Electronics

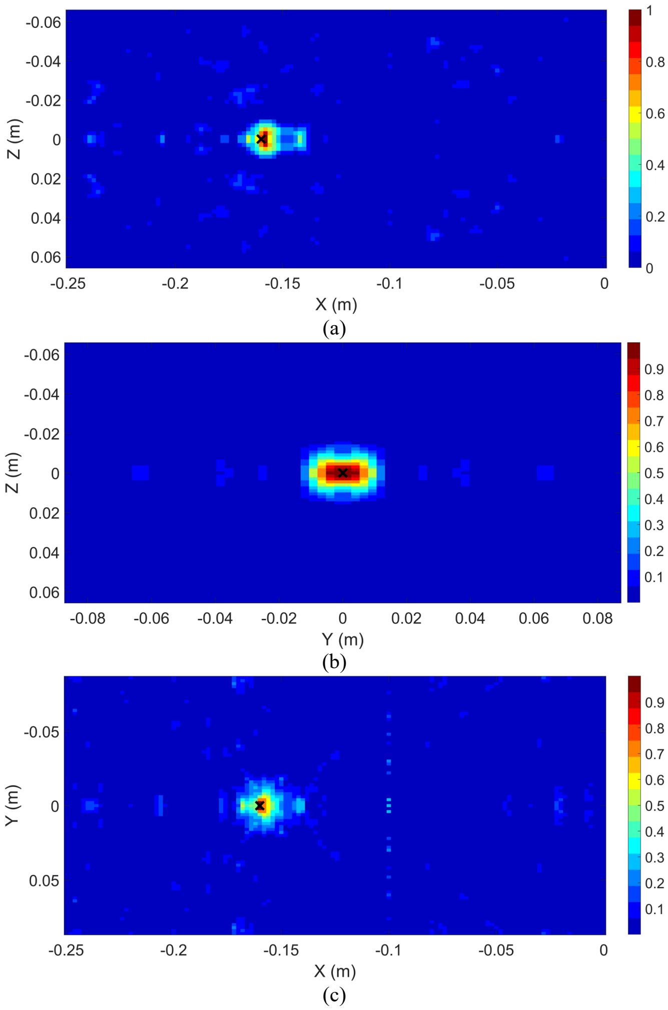

Fig. 13. Distribution of the electric field power at the focusing time slice. The black cross represents the actual location of the source, (a) x-z plane, (b) y-z plane, and (c) x-y plane.

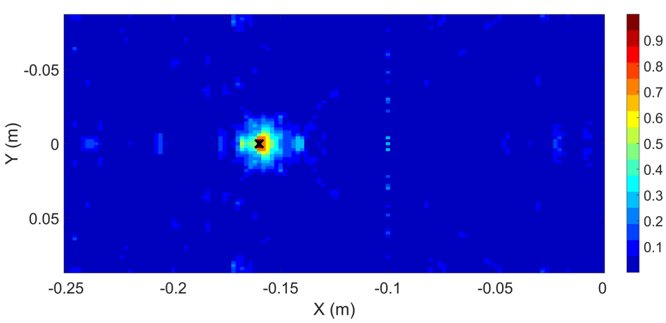

Fig. 14. Distribution of the electric field power at the focusing time slice for an inclined monopole antenna. The black cross represents the actual location of the source.

The first antenna is considered as an EMI source and the second antenna acts as a probe. In this example, as can be seen in Fig. 11b, the EMI source and probe are attached to the cavity. Note that, although we perform our validation test in the frequency domain, the same results are expected in the time domain by applying the inverse Fourier transform. Fig. 12 shows a comparison of the experimentally obtained S_{21} scattering parameter versus CST-MWS simulations. The observed results show agreement between the CST-MWS and the VNA results for the transfer function (Fourier transform of the impulse

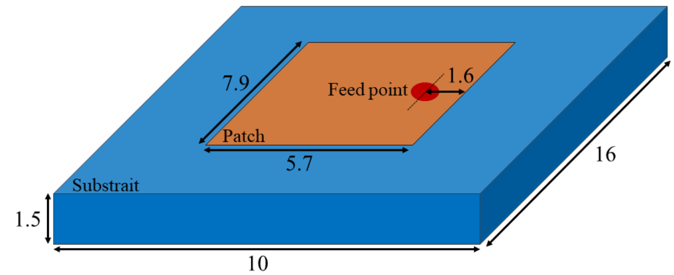

Fig. 15. One unit cell of the considered printed circuit board modeled in the CST-MWS environment. Two-dimensional conducting patch on a dielectric substrate with a conducting ground plane at the bottom (not visible in the figure). All dimensions are in mm.

response) from the source to the sensor in the linear, time-invariant cavity. This lends support to the CST-MWS simulations for validation of the realistic cavity. In other words, this verification shows that the impulse response of the time-invariant linear system simulated by CST-MWS and the measurement using VNA are in good agreement. We can therefore use the CSTMWS simulation results for the forward and backward steps.

2) EMI Source Localization in 3D Cavity for Simple Monopole Antenna

In this section, we assume a monopole antenna as the EMI source at point (-0.16, 0.0, 0.0) m, and a monopole antenna as a probe at (-0.10, 0.0, 0.0) m in the assumed cavity.

In the following simulations, the excitation source is a Gaussian pulse with 10 GHz bandwidth. The length of the monopole antennas is 5.7 mm.

The TR process as described in Section II is applied. The distribution of the electric field power density is calculated by way of CST-MWS and it is depicted in Fig. 13. This figure shows the distribution of the electric field power at the focusing time slice for (a) the x-z plane, (b) the y-z plane, and (c) the x-y plane. The black cross represents the actual location of the source. As we can see in Fig. 13a, the error in finding the location of the source in the x-z plane is one mesh-cell (2 mm). In the other planes, the error is zero. The simulation shows that the proposed method can be used to find with high accuracy (2 mm) the location of the source using only one probe antenna. Our analysis also shows that the method is robust to changes in the respective polarizations of the dipole antennas. Fig. 14 shows the distribution of the electric field power when the orientation of the first antenna is set to 45 degrees relative to the *z*-axis. As can be seen, the method is still able to accurately locate the source (the location error is again one mesh cell, 2mm). Comparing Fig. 13c and 14 reveals that the polarization of the source does not affect the perfermonce of the proposed method in the studied case. If the polarization of the receiving antenna is at right angles to the source polarization, it is obvious that no signal can be recorded by the receiving antenna. To overcome this problem one can peform the measurement in all three possible polarizations.

3) EMI Source Localization in 3D Cavity for microstrip Board

In this subsection, we study the case of a microstrip printed circuit board (PCB) with multiple elements placed inside the

This article has been accepted for publication in a future issue of this journal, but has not been fully edited. Content may change prior to final publication. Citation information: DOI 10.1109/TIE.2019.2962460, IEEE Transactions on Industrial Electronics

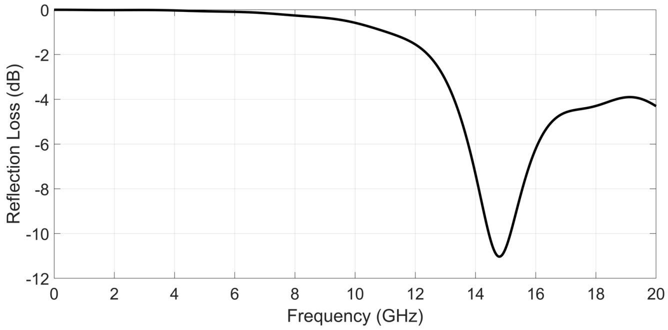

Fig. 16. Reflection loss of the considered microstrip board.

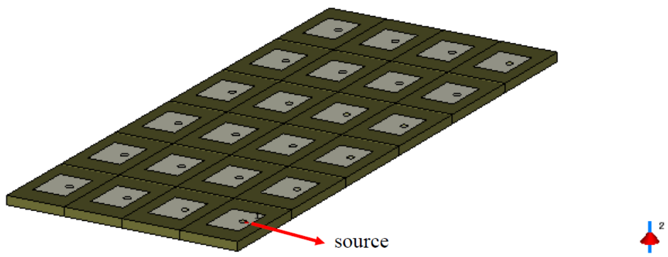

Fig. 17. Assumed printed circuit board with its 24 unit cells. The front left board, excited with a Gaussian pulse, is the EMI source to be located.

model of the cavity. We demonstrate that the proposed time reversal technique can detect and locate the PCB emitting element with very good accuracy.

The PCB considered as the device under test (DUT) has 24 unit cells. It needs to be diagnosed by locating an EMI source on it. Each unit cell of our PCB is a simple microstrip board. A schematic of each unit cell is shown in Fig. 15. The size of the microstrip patch is 7.90×5.69 mm^2. The thickness of the substrate is 1.5 mm and its relative permittivity is 2.1. A 50 Ω coaxial feed is used to excite the microstrip board and it is placed at 1.2 mm off-axis from the center of the patch as shown in Fig. 15. A plot of the reflection loss as a function of frequency for the unit cell (microstrip) can be seen in Fig. 16. As can be seen in that figure, the reflection loss of the microstrip antenna in a narrow frequency band around 15 GHz is lower than -10 dB, which means that the microstrip antenna does not radiate efficiently at 10 GHz compared to 15 GHz. This allows us to test the proposed method in frequency ranges at which the EMI source does not radiate efficiently. It is obvious that in the case of more efficient radiation, the proposed method can work better.

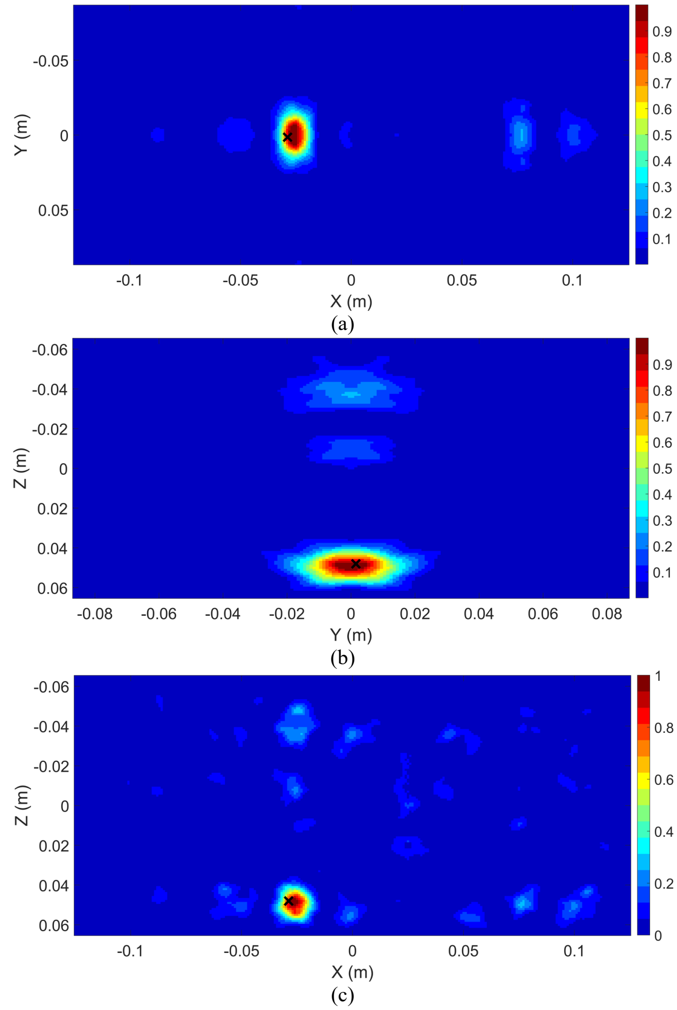

Fig. 19. Distribution of the electric field power at the focusing time slice. The bandwidth of the EMI source is 10 GHz. The black cross represents the actual location of the source, (a) x-z plane, (b) y-z plane, and (c) x-y plane.

The overall printed circuit board including the 24 unit cells next to each other is depicted in Fig. 17. We consider here two case studies in which one unit cell (front-left corner) is excited by a Gaussian pulse with an upper frequency cutoff of either 5 GHz or 10 GHz. A dipole antenna with a length of 5.7 mm is considered as a probe as shown in Fig. 17. The recorded signal via the dipole antenna is time reversed and back injected into the medium. The entropy criterion is applied to obtain the proper time slice.

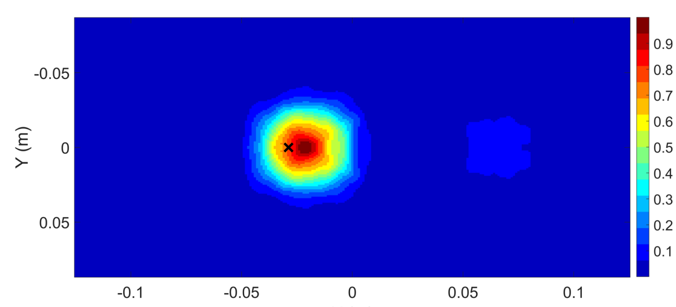

Fig. 18. Distribution of the electric field power in the x-y plane at the focusing time slice. The bandwidth of the EMI source is 5 GHz. The black cross represents the actual location of the source.

This article has been accepted for publication in a future issue of this journal, but has not been fully edited. Content may change prior to final publication. Citation information: DOI 10.1109/TIE.2019.2962460, IEEE Transactions on Industrial Electronics

Fig. 18 shows the distribution of the electric field power in the x-z plane at the focusing time slice when the EMI source is excited by a Gaussian pulse with a bandwidth of 5 GHz. As it can be seen, the proposed method can detect the emitting unit cell. Considering the exact location of the coaxial feed point (center of the feed), the proposed method yields a location estimation error of 7.5 mm.

Fig. 19 shows the distribution of the electric field power at the focusing time slice when the EMI source is excited by a Gaussian pulse with a bandwidth of 10 GHz. As it can be seen, the proposed method is again able to detect the emitting unit cell. Considering again the coaxial feed exact location point (center of the feed), the proposed method yields an accuracy of 3.3 mm. As expected, by increasing the EMI source radiation bandwidth, the accuracy of this method is improved thanks to the better focusing properties of TRCs at higher frequencies.

V. Conclusion

In this paper, we proposed a novel method to detect and locate EMI sources by exploiting the spatial and temporal focusing properties of Time Reversal. We proposed to insert the device under test in a full metallic cavity to use its rich multipath environment to achieve a high focusing effect. We proposed a new perspective based on image theory to show that Time Reversal Cavities (TRCs) can provide highly focused images of sources with a single sensor since the electromagnetic behavior of the single sensor within a cavity is equivalent to that of an infinite number of sensors in free space. This new insight was tested via numerical FDTD simulations. Furthermore, as a proof of concept, 2D numerical simulations were used to demonstrate the ability of TRCs to locate EMI sources. The minimum entropy criterion was used in the time reversal process to obtain the focusing time. We showed that EMI sources can be located using only a single sensor. The proposed EMI source localization method does not need any form of scanning compared to former conventional near-field and far-field probing schemes and it can overcome their difficulties in this respect.

We validated our simulation procedure by comparing the cavity's source-to-sensor transfer function obtained from simulations against the same parameter obtained via measurements. The frequency response of the cavity was measured using a Vector Network Analyzer (VNA) and it was calculated by simulation using a simple model in CST-MWS.

Finally, we used a realistic 3D scenario with the presence of a large board including microstrip patches and we showed that the location of an EMI source can be successfully identified. The performance of the method was tested against changes in polarization of the source and low efficiency radiation of the EMI sources. The proposed technique is much simpler and cost effective than EMI tests in anechoic chambers or other near field or far field scanning methods.

References

[1] B. Archambeault, C. Brench, and S. Connor, "Review of Printed-Circuit-Board Level EMI/EMC Issues and Tools," *IEEE Trans. Electromagn. Compat.*, vol. 52, no. 2, pp. 455–461, May 2010.

[2] H. V. Poor and G. W. Wornell, *Wireless Communications: Signal Processing Perspectives*. Prentice Hall, 1998.

[3] I. F. Akyildiz, W. Su, Y. Sankarasubramaniam, and E. Cayirci, "Wireless sensor networks: a survey," *Comput. Networks*, vol. 38, no. 4, pp. 393–422, Mar. 2002.

[4] M. I. Skolnik, *Introduction to Radar Systems*. McGraw-Hill, 2000.

[5] R. O. Nielsen, *Sonar signal processing*. Boston : Artech House, 1991.

[6] E. A. Robinson and S. Treitel, *Geophysical Signal Analysis*. Prentice Hall, 1980.

[7] P. Strumillo, *Advances in Sound Localization*. InTech, 2011.

[8] Y. Sun, J. Chen, C. Yuen, and S. Rahardja, "Indoor Sound Source Localization With Probabilistic Neural Network," *IEEE Trans. Ind. Electron.*, vol. 65, no. 8, pp. 6403–6413, Aug. 2018.

[9] J. P. Lanslots, F. Deblauwe, and K. Janssens, "Selecting Sound Source Localization Techniques for Industrial Applications," *Sound Vib.*, vol. 44(6), 2010.

[10] F. Deng, S. Guan, X. Yue, X. Gu, J. Chen, J. Lv, and J. Li, "Energy-Based Sound Source Localization with Low Power Consumption in Wireless Sensor Networks," *IEEE Trans. Ind. Electron.*, vol. 64, no. 6, pp. 4894–4902, Jun. 2017.

[11] F. Rachidi, M. Rubinstein, and M. Paolone, *Electromagnetic Time Reversal: Application to EMC and Power Systems*. 2017.

[12] H. Karami, A. Mostajabi, M. Azadifar, Z. Wang, M. Rubinstein, and F. Rachidi, "Locating Lightning Using Electromagnetic Time Reversal : Application of the Minimum Entropy Criterion," in *International Symposium on Lightning Protection (XV SIPDA)*, 2019.

[13] J. J. H. Wang, "An Examination of the Theory and Practices of Planar Near-field Measurement," *IEEE Trans. Antennas Propag.*, vol. 36, no. 6, pp. 746–753, 1988.

[14] H. He, P. Maheshwari, and D. J. Pommerenke, "The Development of an EM-Field Probing System for Manual Near-Field Scanning," *IEEE Trans. Electromagn. Compat.*, vol. 58, no. 2, pp. 356–363, Apr. 2016.

[15] P. Maheshwari, H. Kajbaf, V. V. Khilkevich, and D. Pommerenke, "Emission Source Microscopy Technique for EMI Source Localization," *IEEE Trans. Electromagn. Compat.*, vol. 58, no. 3, pp. 729–737, Jun. 2016.

[16] M. Fink, D. Cassereau, and A. Derode, "Time-reversed mirrors," *J. Phys. D. Appl. Phys.*, vol. 26, p. 1333, 1993.

[17] M. Fink, "Time Reversed Acoustics," *Phys. Today*, vol. 50, no. 3, pp. 34–40, Mar. 1997.

[18] A. Derode, A. Tourin, J. De Rosny, M. Tanter, S. Yon, and M. Fink, "Taking Advantage of Multiple Scattering to Communicate with Time-Reversal Antennas," *Phys. Rev. Lett.*, vol. 90.1, 2003.

[19] D. Cassereau and M. Fink, "Time-reversal of ultrasonic fields. III. Theory of the closed time-reversal cavity," *IEEE Trans. Ultrason. Ferroelectr. Freq. Control*, vol. 39, no. 5, pp. 579–592, Sep. 1992.

[20] A. P. Sarvazyan, L. Fillinger, and L. R. Gavrilov, "A comparative study of systems used for dynamic focusing of ultrasound," *Acoust. Phys.*, vol. 55, no. 4–5, pp. 630–637, Oct. 2009.

[21] G. Lerosey, J. de Rosny, A. Tourin, A. Derode, G. Montaldo, and M. Fink, "Time Reversal of Electromagnetic Waves," *Phys. Rev. Lett.*, vol. 92, no. 19, p. 193904, May 2004.

[22] R. Carminati, R. Pierrat, J. de Rosny, and M. Fink, "Theory of the time reversal cavity for electromagnetic fields," *Opt. Lett.*, vol. 32, no. 21, p. 3107, Nov. 2007.

[23] I. El Baba, S. Lallechere, and P. Bonnet, "Electromagnetic Time-Reversal for reverberation chamber applications using FDTD," in *2009 International Conference on Advances in Computational Tools for Engineering Applications*, 2009, pp. 157–162.

[24] H. Moussa, A. Cozza, and M. Cauterman, "A Novel Way of Using Reverberation Chambers Through Time-Reversal," in *ESA Workshop on Aerospace EMC (ESA'09)*, 2009, no. April, p. pp.10-2.

[25] Xiaoyin Xu, E. L. Miller, and C. M. Rappaport, "Minimum entropy regularization in frequency-wavenumber migration to localize subsurface objects," *IEEE Trans. Geosci. Remote Sens.*, vol. 41, no. 8, pp. 1804–1812, Aug. 2003.

[26] M. Fink, J. de Rosny, G. Lerosey, and A. Tourin, "Time-reversed waves and super-resolution," *Comptes Rendus Phys.*, vol. 10, no. 5, pp. 447–463, Jun. 2009.

[27] M. Fink, G. Montaldo, and M. Tanter, "Time-Reversal Acoustics in Biomedical Engineering," *Annu. Rev. Biomed. Eng.*, vol. 5, no. 1, pp. 465–497, Aug. 2003.

[28] R. A. Wiggins, "Minimum entropy deconvolution," *Geoexploration*, vol. 16, no. 1–2, pp. 21–35, Apr. 1978.

This article has been accepted for publication in a future issue of this journal, but has not been fully edited. Content may change prior to final publication. Citation information: DOI 10.1109/TIE.2019.2962460, IEEE Transactions on Industrial Electronics

Hamidreza Karami received the B.S. degree in electrical engineering from Bu-Ali Sina University, Hamedan, Iran, in 2004 and the M.S. and Ph.D. degrees in telecommunications from Amirkabir University of Technology, Tehran, Iran, in 2008 and 2013, respectively. He was with École Polytechnique, Fédérale de Lausanne (EPFL), Lausanne, Switzerland, in June 2013 as a Visiting Scientist. He is currently an Assistant Professor of electrical engineering with Bu-Ali Sina University, Hamedan, Iran. He is currently visiting scientist at EPFL from 2019. His research interests include electromagnetic compatibility (EMC), computational methods in electromagnetics, microwave nondestructive testing techniques, and time reversal.

Mohammad Azadifar (M'18) received the B.S. and M.S (with distinction) degrees in electrical engineering from the Amirkabir University of Technology (Tehran Polytechnic), Tehran, Iran, in 2005 and 2009, respectively. He received the Ph.D. degree in Electrical Engineering from the Swiss Federal Institute of Technology (EPFL), Lausanne, Switzerland, in 2018. In 2018, he joined the University of Applied Sciences of Western Switzerland, Yverdon-les-Bains, Switzerland, where he is currently researcher at the Information and Communication Technologies institute team. He has authored or co-authored over 40 scientific journal and conference papers. His research interests include electromagnetic compatibility (EMC), time reversal, and lightning.

Amirhossein Mostajabi (Student Member 2009) received the B.Sc. and M.Sc. degrees in electrical engineering from the University of Tehran, Tehran, Iran, in 2011 and 2014, respectively. From 2009 to 2017, he has been with the High Voltage Institute of University of Tehran as a research assistant. In 2017, he joined the Electromagnetic Compatibility Laboratory of Swiss Federal Institute of Technology (EPFL) where he is currently pursuing the Ph.D. degree in electrical engineering. His main research interests include numerical computation of electromagnetic fields, lightning electromagnetics, and applied machine learning.

Pierre Favrat was born in Lausanne, Switzerland, on May 19th, 1967. He received the M.S. degree in 1994 and the Ph.D. degree in 1998 for his work on integrated circuits for electrostatic actuators from the Swiss Federal Institute of Technology (EPFL), Lausanne, Switzerland.

From 1998 to 2000, he held the position of analog RF designer at STMicroelectronics. In 2001, he founded Xceive Corp., Santa Clara, California, a company focused on building integrated tuners for television broadcasts, and became its CEO. In 2010, he joined Lemoptix SA in Lausanne, Switzerland where he was leading the Engineering team. Since 2012, he is a professor at the University of Applied Science Western Switzerland (HES-SO). His research activities are related to RF antennas, RF circuits and communication technologies.

Marcos Rubinstein (M'84–SM'11–F'14) received the Master's and Ph.D. degrees in electrical engineering from the University of Florida, Gainesville, FL, USA, in 1986 and 1991, respectively.

In 1992, he joined the Swiss Federal Institute of Technology, Lausanne, Switzerland, where he was involved in the fields of electromagnetic compatibility and lightning. In 1995, he was with Swisscom, where he worked in numerical electromagnetics and EMC. In 2001, he moved to the University of Applied Sciences of Western Switzerland HES-SO, Yverdon-les-Bains, where he is currently a full Professor, head of the advanced Communication Technologies Group and a member of the IICT Institute Team. He is the author or coauthor of more than 300 scientific publications in reviewed journals and international conferences. He is also the coauthor of seven book chapters and one of the editors of a book on Electromagnetic Time Reversal. He served as the Editor-in-Chief of the Open Atmospheric Science Journal and he currently serves as an Associate Editor of the IEEE Transactions on Electromagnetic Compatibility.

Prof. Rubinstein received the best Master's Thesis award from the University of Florida. He received the IEEE achievement award and he is a co-recipient of the NASA's Recognition for Innovative Technological Work award. He is also the recipient of the ICLP Karl Berger Award. He is a Fellow of the IEEE and of the SUMMA Foundation, a member of the Swiss Academy of Sciences and of the International Union of Radio Science.

Farhad Rachidi (M'93–SM'02–F'10) received the M.S. degree and the Ph.D. degree in electrical engineering from the Swiss Federal Institute of Technology, Lausanne, Switzerland, in 1986 and 1991, respectively. He was with the Power Systems Laboratory, Swiss Federal Institute of Technology, until 1996. In 1997, he joined the Lightning Research Laboratory, University of Toronto, Toronto, ON, Canada. From 1998 to 1999, he was with Montena EMC, Rossens, Switzerland. He is currently a Titular Professor and the Head of the EMC Laboratory with the Swiss Federal Institute of Technology, Lausanne, Switzerland. He has authored or co-authored over 200 scientific papers published in peer-reviewed journals and over 400 papers presented at international conferences.

Dr. Rachidi is currently a member of the Advisory Board of the IEEE Transactions on Electromagnetic Compatibility and the President of the Swiss National Committee of the International Union of Radio Science. He has received numerous awards including the 2005 IEEE EMC Technical Achievement Award, the 2005 CIGRE Technical Committee Award, the 2006 Blondel Medal from the French Association of Electrical Engineering, Electronics, Information Technology and Communication (SEE), the 2016 Berger Award from the International Conference on Lightning Protection, the Best Paper Award of the IEEE Transactions on EMC (2016 and 2018), and the Motohisa Kanda Award for the most cited paper of the IEEE Transactions on EMC (2012-2016 and 2014-2018). In 2014, he was conferred the title of Honorary Professor of the Xi'an Jiaotong University in China. He served as the Vice-Chair of the European COST Action on the Physics of Lightning Flash and its Effects from 2005 to 2009, the Chairman of the 2008 European Electromagnetics International Symposium, the President of the International Conference on Lightning Protection from 2008 to 2014, the Editor-in-Chief of the Open Atmospheric Science Journal (2010-2012) and the Editor-in-Chief of the IEEE Transactions on Electromagnetic Compatibility from 2013 to 2015. He is a Fellow of the IEEE and of

This article has been accepted for publication in a future issue of this journal, but has not been fully edited. Content may change prior to final publication. Citation information: DOI 10.1109/TIE.2019.2962460, IEEE Transactions on Industrial Electronics

the SUMMA Foundation, and a member of the Swiss Academy of Sciences.